Int. J. Solids Structures Vol. 22, No. 1, pp. 23–37, 1986
Printed in Great Britain.

0020-7683/86 $3.00 + .00

APPLICATION OF BODY FORCE METHOD TO THE ANALYSIS OF STRESS CONCENTRATION OF AN AXI-SYMMETRIC BODY UNDER BENDING: I. BASIC THEORY AND APPLICATION TO SEVERAL SIMPLE PROBLEMS

Y. MURAKAMI†, N. NODA‡ and H. NISITANI
Department of Mechanics and Strength of Solids, Faculty of Engineering, Kyushu University, Fukuoka 812, Japan

(*Received* 19 *December* 1983; *replacement received* 22 *April* 1985)

Abstract—The general theory is established for the application of the body force method to the stress concentration analysis of an axi-symmetrical body under bending. Determination of fundamental solutions in bending are not self-evident as in tension or torsion problems. However, comparing the boundary conditions to be satisfied along circumferential position of imaginary boundary and stress fields due to the body force distributed trigonometrically along a ring around the axis, it is found that three kinds of fundamental solutions are necessary and sufficient. Thus, the axi-symmetrical problem could be treated in the similar manner as two-dimensional problems.

For example, problems of a spheroidal cavity and a troidal cavity in an infinite body under bending are solved numerically. The error in the former problem is less than 0.07%. The results of the latter problem agree with the exact solution in the two limiting cases; a deep hyperbolic notch and two dimensional elliptic hole.

1. INTRODUCTION

The stress analysis of an axi-symmetric body under bending is in general more difficult than tension and torsion. The recent development of the finite element method (FEM) has enabled us to obtain the approximate solution for almost all elasticity problems. However, actually FEM is not suitable for systematic calculation of the accurate stress concentration factors for various combinations of shapes and dimensions. A typical problem of an axi-symmetric body under bending, is the stress concentration problem of the cylindrical bar with a circumferential notch which is often used in the rotating bending fatigue test. Neuber[1–3] determined approximately the stress concentration factors (SCF) of this problem. However, the exact solutions have been expected for more advanced researches on fatigue and fracture strength of notched specimens[4].

In the present paper, the basic theory of the body force method[5, 6] is developed for the stress concentration analysis of an axi-symmetrical body and a couple of examples, a spheroidal cavity and a troidal cavity, are solved. The accuracies in the case of spheroidal cavity and in the limiting case of a troidal cavity are discussed in comparison with Neuber's exact solutions. First of all, the theories of tension[7, 8] and torsion[9] analyses of an axi-symmetrical body are reviewed, and then the method of finding the three fundamental solutions that are necessary for the satisfaction of boundary conditions will be explained. Since such fundamental solutions cannot be found self-evidently in bending problems unlike tension and torsion problems, the stress fields due to various fundamental solutions must be investigated carefully. However, once the computer program is completed using the fundamental solutions, the accurate stress concentration factors for the systematic change of shapes and dimensions can be easily obtained and the tables and charts for design can also be made.

† Professor.

‡ Graduate student. Current position and address: Lecturer, Department of Mechanical Engineering, Kyushu Institute of Technology, Tobata, Kitakyushu, 812 Japan.

2. THEORY

The principle of the body force method is simply based on the superposition of the stress field (Green's function) due to a point force applied in the infinite or semi-infinite body. The densities of the point forces distributed along imaginary boundaries are determined considering the boundary conditions. However, the method of superposition or the way of point force distribution must be carefully chosen considering the physical meaning of the stress and displacement field. The basic principle of the body force method is explained in Ref. [5, 6]. In the present paper, the application of the method is explained with emphasis on the three dimensional bending analysis of an axially symmetric body.

2.1. *Fundamental solution for the analysis of tension and torsion problem*

The body force method was originally proposed as the numerical method solving two-dimensional stress problem[5]. Although in principle it can be applied to arbitrary problems, the special improvement and extension in individual problems are necessary in order to obtain accurate results. In the early stage of the development, the body force method has been applied to various two-dimensional problems in which (i) the fundamental solution is a stress field due to a point force applied at a point of an infinite plate and (ii) the prospective boundaries are divided into finite straight or curved divisions, the midpoints of which are used for the representative points where the stress boundary conditions are satisfied. The same method was applied to several three-dimensional axi-symmetrical problems[7–9], in which (i)* the stress field due to the continuously distributed point forces along a ring around the axis of symmetry was used as the fundamental solutions instead of (i).

It is easily understood that the point force continuously distributed in radial and axial direction (Fig. 1 (a), (b)) along a ring around the axis of symmetry gives the fundamental solutions for tension problems[7, 8] and those distributed in circumferential direction (Fig. 1 (c)) give the fundamental solutions for torsion problems[9]. The procedure (ii) in two-dimensional case can also be used, because if the boundary conditions is satisfied at one point (the marked point ○ in Fig. 1(d)) of the circumference, it is naturally satisfied at all points of the circumference from axial symmetry. Then, the extension from plane problem to axially symmetric problem is established completing two procedure, (i)* distributing point forces continuously along a ring around the axis of symmetry, and (ii)* satisfying the boundary conditions at all points of one circumference.

Thus, if the satisfaction of the boundary conditions at all points of one circumference is possible in bending problems of an axially symmetric body, the calculation procedure becomes almost similar to those previously adopted. It depends on whether we can find the fundamental solutions, instead of (i) and (i)*, that satisfy the axially asymmetric boundary conditions at all points of one circumference. However, unlike plane and axially symmetric problems, such fundamental solution can not be found self-evidently. The properties of the fundamental solutions required in the bending analysis of an axially symmetric body are discussed in the next section.

2.2. *The fundamental solutions required in the analysis of an axi-symmetrical body under bending*

Imagine an infinite body subjected to bending moment at infinity. If we take z axis as the axis of symmetry and apply the bending moment around the radial axis of $\theta = \pi/2$ in Figs. 2 and 3, the stresses far from the origin are expressed in the following equation.

$$\begin{aligned} \sigma_z &= \sigma_0 \frac{r}{a} \cos\theta \\ \sigma_r &= \sigma_\theta = \tau_{rz} = \tau_{r\theta} = \tau_{\theta z} = 0, \end{aligned} \tag{1}$$

where σ_0 is the constant which corresponds to the magnitude of bending stress and a

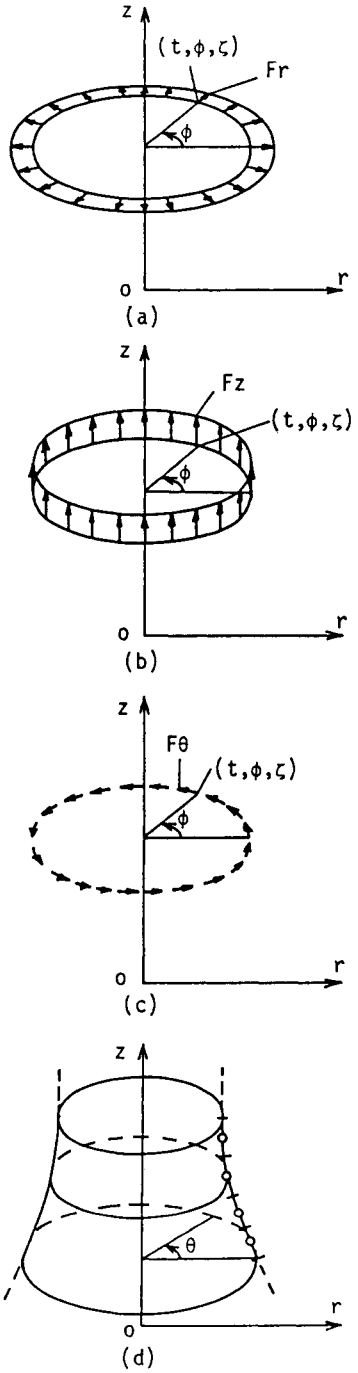

Fig. 1. Fundamental solution for the analysis of tension ((a) and (b)) and torsion (c) problems and the prospective boundaries divided into finite divisions (d).

is the representative dimension. Since the stress σ_z at infinity varies in the type of cos θ, the stress σ_z induced by point forces distributed in z-direction (the ring force; a fundamental solution) should also vary in the type of cos θ on the circumference of radius r and height z. Then, we suppose the intensities of two ring forces in the form of cos ϕ; one is in the z-direction (Fig. 2) and the other is in the r-direction (Fig. 3) that are applied on the circumference of radius t and z-coordinate ζ. (t, ϕ, ζ) is used as the cylindrical coordinates of the points where the forces are applied. In addition to the ring force with intensity of cos ϕ in radial direction is also necessary as the fundamental solution, because the stresses in the r-direction induced by the ring force

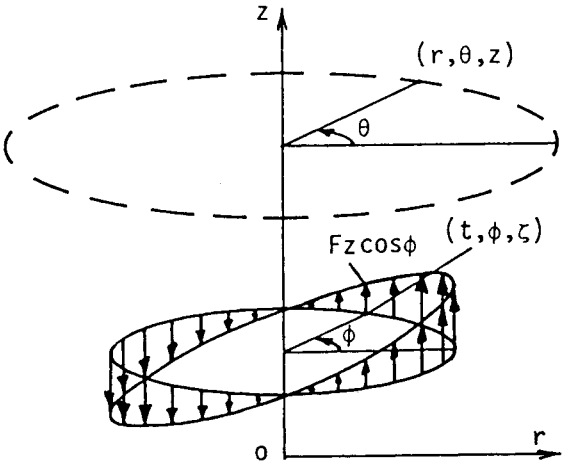

Fig. 2. A ring force with intensity cos ϕ in the z-direction.

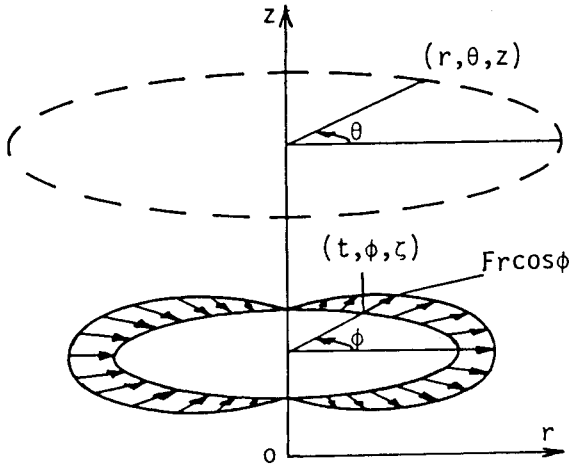

Fig. 3. A ring force with intensity cos ϕ in the r-direction.

in the z-direction must be cancelled. Thus, we can find that the ring force in either direction induces the stresses as the type of eqn (2) at (r, θ, z). (r, θ, z) is the coordinate where the stresses are expected to be calculated.

$$\begin{aligned} \sigma_r &= f_1(r, t, z, \zeta)\cos\theta, \quad \sigma_\theta = f_2(r, t, z, \zeta)\cos\theta, \quad \sigma_z = f_3(r, t, z, \zeta)\cos\theta \\ \tau_{rz} &= f_4(r, t, z, \zeta)\cos\theta, \quad \tau_{r\theta} = f_5(r, t, z, \zeta)\sin\theta, \quad \tau_{\theta z} = f_6(r, t, z, \zeta)\sin\theta. \end{aligned} \tag{2}$$

Equation (2) indicates that the stresses at (r, θ, z) in the infinite body can be determined by multiplying those at $(r, 0, z)$ by cos θ. And we can see that the normal stresses σ_n and the shearing stress τ_{nt} at a point of an arbitrary curved surface imagined in the infinite body, also vary in the type of cos θ along the circumference as shown in eqn (3).

$$\begin{aligned} \sigma_n &= \sigma_r \cos^2\psi_1 + \sigma_z \sin^2\psi_1 + 2\tau_{rz}\sin\psi_1\cos\psi_1 \\ &= (f_1\cos^2\psi_1 + f_3\sin^2\psi_1 + 2f_4\sin\psi_1\cos\psi_1)\cos\theta \\ \tau_{nt} &= (-\sigma_r + \sigma_z)\sin\psi_1\cos\psi_1 + \tau_{rz}(\cos^2\psi_1 - \sin^2\psi_1) \\ &= \{(-f_1 + f_3)\sin\psi_1\cos\psi_1 + f_4(\cos^2\psi_1 - \sin^2\psi_1)\}\cos\theta \end{aligned} \tag{3}$$

where, ψ_1 is the angle between the r-axis and the normal direction of the surface. Therefore, if the condition $\sigma_n = \tau_{nt} = 0$ are satisfied at $r = r$, $\theta = 0$, the same boundary

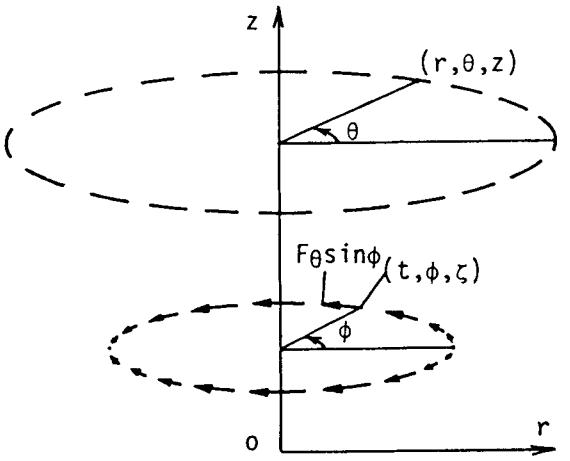

Fig. 4. A ring force with intensity sin ϕ in the θ-direction.

conditions are automatically satisfied at all points of $\theta \neq 0$ on the same radius $r = r$. Concerning the condition σ_n and τ_{nt}, it looks like that the combinations of these two kinds of ring forces applied in z and r direction are sufficient for the satisfaction of the boundary conditions. However, actually the combinations of ring forces of the types of Figs. 2 and 3 are insufficient, because the application of them induces the shearing stress $\tau_{n\theta}$ (i.e. $\tau_{r\theta}$ and $\tau_{\theta z}$) at the boundary which must become the free surface. The shearing stress $\tau_{n\theta}$ is expressed by the following equation.

$$\begin{aligned} \tau_{n\theta} &= \tau_{r\theta} \cos \psi_1 + \tau_{\theta z} \sin \psi_1 \\ &= (f_5 \cos \psi_1 + f_6 \sin \psi_1) \sin \theta. \end{aligned} \tag{4}$$

As seen from eqn (4), $\tau_{n\theta}$ varies in the type of sin θ on the radius $r = r$. Then, it becomes necessary to apply the tangential ring force that changes in type of sin ϕ on the radius $r = r$ as shown in Fig. 4. The application of the ring force of the type of Fig. 4 newly induces the stresses σ_r, σ_z and τ_{rz} that should have the type of eqn (2) again in order to satisfy the boundary conditions. It is confirmed that the application of the ring forces of the type of Fig. 4 induces the stress field in the type of eqn (2).

The above discussion leads us to the conclusion that the three types of ring forces in Figs. 2–4 are necessary and sufficient for the satisfaction of the boundary conditions of the bending problems of axially symmetric body. In this way, we can use the calculation procedure similar to tension or torsion problems. Therefore, we have only to notice the stresses (σ_r, σ_θ, σ_z, τ_{rz}) at the section $\theta = 0$ and the stresses ($\tau_{r\theta}$, $\tau_{\theta z}$) at the section $\theta = \pi/2$ in order to satisfy the boundary conditions, that is, we have only to treat the functions f_1–f_6 in eqn (2) that correspond to the amplitudes of the stresses along circumferences. Thus, the numerical procedure has been established as similar one to two-dimensional cases and the numbers of unknowns are three in one division of Fig. 1(d).

3. THE FUNDAMENTAL SOLUTIONS

When a point force acts at a point (t, ϕ, ζ) in an infinite body, the stresses at (r, θ, z) are given by eqn (5)[10], where (F_r, F_θ, F_z) mean the forces and ($\sigma_r^{F_r}$–$\tau_{\theta z}^{F_r}$, $\sigma_r^{F_\theta}$–$\tau_{\theta z}^{F_\theta}$, $\sigma_r^{F_z}$–$\tau_{\theta z}^{F_z}$) do stresses in r, θ and z direction.

$$\begin{aligned} \sigma_r^{F_r} &= B_1[[(1 - 2\nu)R^{-3}[-r \cos(\varphi - \theta) + t\{2 \cos^2(\varphi - \theta) - 1\}] \\ &\quad - 3R^{-5}\{r \cos(\varphi - \theta) - t\}\{r - t \cos(\varphi - \theta)\}^2]] \\ \sigma_\theta^{F_r} &= B_1[[(1 - 2\nu)R^{-3}[r \cos(\varphi - \theta) - t\{2 \cos^2(\varphi - \theta) - 1\}] \\ &\quad - 3R^{-5}\{-r \cos(\varphi - \theta) + t\}t^2 \sin^2(\varphi - \theta)]] \end{aligned}$$

$$
\begin{aligned}
\sigma_z^{F_r} &= B_1[(1-2\nu)R^{-3} - 3(z-\zeta)R^{-5}]\{r\cos(\varphi-\theta) - t\} \\
\tau_{rz}^{F_r} &= B_1(z-\zeta)[-(1-2\nu)R^{-3}\cos(\varphi-\theta) - 3R^{-5}\{r\cos(\varphi-\theta) - t\} \\
&\quad \times \{r - t\cos(\varphi-\theta)\}] \\
\tau_{r\theta}^{F_r} &= B_1[(1-2\nu)R^{-3}\sin(\varphi-\theta)\{2t\cos(\varphi-\theta) - r\} \\
&\quad + 3R^{-5}t\sin(\varphi-\theta)\{r\cos(\varphi-\theta) - t\}\{r - t\cos(\varphi-\theta)\}] \\
\tau_{\theta z}^{F_r} &= B_1(z-\zeta)[-(1-2\upsilon)R^{-3}\sin(\varphi-\theta) + 3R^{-5}\{r\cos(\varphi-\theta) - t\} \\
&\quad t\sin(\varphi-\theta)]
\end{aligned}
\tag{5a}
$$

$$
\begin{aligned}
\sigma_r^{F_\theta} &= B_2[(1-2\nu)R^{-3}\sin(\varphi-\theta)\{r - 2t\cos(\varphi-\theta)\} \\
&\quad + 3R^{-5}r\sin(\varphi-\theta)\{r - t\cos(\varphi-\theta)\}^2] \\
\sigma_\theta^{F_\theta} &= B_2[(1-2\nu)R^{-3}\sin(\varphi-\theta)\{-r + 2t\cos(\varphi-\theta)\} + 3R^{-5}rt^2\sin^3(\varphi-\theta)] \\
\sigma_z^{F_\theta} &= B_2[(1-2\nu)R^{-3} - 3(z-\zeta)^2R^{-5}]\{-r\sin(\varphi-\theta)\} \\
\tau_{rz}^{F_\theta} &= B_2(z-\zeta)[(1-2\nu)R^{-3}\sin(\varphi-\theta) + 3R^{-5}r\sin(\varphi-\theta)\{r - t\cos(\varphi-\theta)\}] \\
\tau_{r\theta}^{F_\theta} &= B_2[\![-(1-2\nu)R^{-3}[r\cos(\varphi-\theta) - t\{2\cos^2(\varphi-\theta) - 1\}] \\
&\quad - 3R^{-5}rt\sin^2(\varphi-\theta)\{r - t\cos(\varphi-\theta)\}]\!] \\
\tau_{\theta z}^{F_\theta} &= B_2(z-\zeta)\{-(1-2\nu)R^{-3}\cos(\varphi-\theta) - 3R^{-5}rt\sin^2(\varphi-\theta)\}
\end{aligned}
\tag{5b}
$$

$$
\begin{aligned}
\sigma_r^{F_z} &= B_3(z-\zeta)[(1-2\nu)R^{-3} - 3R^{-5}\{r - t\cos(\varphi-\theta)\}^2] \\
\sigma_\theta^{F_z} &= B_3(z-\zeta)[(1-2\nu)R^{-3} - 3R^{-5}t^2\sin^2(\varphi-\theta)] \\
\sigma_z^{F_z} &= B_3(z-\zeta)[-(1-2\nu)R^{-3} - 3R^{-5}(z-\zeta)^2] \\
\tau_{rz}^{F_z} &= B_3\{-(1-2\nu)R^{-3} - 3(z-\zeta)^2R^{-5}\}\{r - t\cos(\varphi-\theta)\} \\
\tau_{r\theta}^{F_z} &= B_3[3(z-\zeta)R^{-5}t\sin(\varphi-\theta)\{r - t\cos(\varphi-\theta)\}] \\
\tau_{\theta z}^{F_z} &= B_3\{-(1-2\nu)R^{-3} - 3(z-\zeta)^2R^{-5}\}\{-t\sin(\varphi-\theta)\}
\end{aligned}
\tag{5c}
$$

$$
B_1 = \frac{F_r}{8\pi(1-\nu)}, \qquad B_2 = \frac{F_\theta}{8\pi(1-\nu)}, \qquad B_3 = \frac{F_z}{8\pi(1-\nu)} \tag{5d}
$$

$$
R^2 = r^2 + t^2 + (z-\zeta)^2 - 2rt\cos(\varphi-\theta). \tag{5e}
$$

In eqn (5), it should be noticed that the forces F_r, F_θ and F_z are applied on the infinitestimal curved area $td\phi ds$ (line element C in Fig. 5) in the following equation

$$
dF_r \propto t\cos\varphi\, d\varphi\, d\zeta, \quad dF_\theta \propto t\sin\varphi\, d\varphi\, dS, \quad dF_z \propto t\cos\varphi\, d\varphi\, dt \tag{5f}
$$

In eqn (5a) and eqn (5c), the stresses (σ_r, σ_θ, σ_z, τ_{rz}) due to F_r and F_z are the even functions of φ' ($= \varphi - \theta$), while the stresses ($\tau_{r\theta}$, $\tau_{\theta z}$) are the odd functions of φ'. On the contrary, in eqn (5b) the stresses (σ_r, σ_θ, σ_z, τ_{rz}) due to F_θ are the odd functions of φ', while the stress ($\tau_{r\theta}$, $\tau_{\theta z}$) are the even functions of φ'. Taking eqn (5f) into consideration, the fundamental solutions ($\sigma_r^{F_r*}$, $\sigma_\theta^{F_r*}$, . . . , $\tau_{\theta z}^{F_z*}$) can be obtained integrating eqn (5a)–eqn (5c) in which F_r, F_θ and F_z are replaced by $t\cos\varphi$ or $t\sin\varphi$ according to eqn (5f). If we notice the following equation,

$$
\begin{aligned}
\cos\varphi &= \cos(\varphi' + \theta) = \cos\varphi'\cos\theta - \sin\varphi'\sin\theta \\
\sin\varphi &= \sin(\varphi' + \theta) = \sin\varphi'\cos\theta + \cos\varphi'\sin\theta
\end{aligned}
\tag{6}
$$

we can see the integration ($\varphi' = 0$–2π) associated with the odd function of φ' vanishes

and we can obtain the stress fields of the type of eqn (2). Finally, the fundamental solutions $\sigma_r^{F_r*}-\rho_{\theta z}^{F_z*}$ are expressed as follows.

$$
\begin{aligned}
\sigma_r^{F_r*} &= \int_0^{2\pi} \sigma_r^{F_r}\, t\cos\varphi'\,d\varphi'\cos\theta, \quad \sigma_\theta^{F_r*} = \int_0^{2\pi} \sigma_\theta^{F_r}\, t\cos\varphi'\,d\varphi'\cos\theta \\
\sigma_z^{F_r*} &= \int_0^{2\pi} \sigma_z^{F_r}\, t\cos\varphi'\,d\varphi'\cos\theta, \quad \tau_{rz}^{F_r*} = \int_0^{2\pi} \tau_{rz}^{F_r}\, t\cos\varphi'\,d\varphi'\cos\theta \\
\tau_{r\theta}^{F_r*} &= -\int_0^{2\pi} \tau_{r\theta}^{F_r}\, t\sin\varphi'\,d\varphi'\sin\theta, \quad \tau_{\theta z}^{Fr*} = -\int_0^{2\pi} \tau_{\theta z}^{F_r}\, t\sin\varphi'\,d\varphi'\sin\theta \\
\sigma_r^{F_\theta*} &= \int_0^{2\pi} \sigma_r^{F_\theta}\, t\sin\varphi'\,d\varphi'\cos\theta, \quad \sigma_\theta^{F_\theta*} = \int_0^{2\pi} \sigma_\theta^{F_\theta}\, t\sin\varphi'\,d\varphi'\cos\theta \\
\sigma_z^{F_\theta*} &= \int_0^{2\pi} \sigma_z^{F_\theta}\, t\sin\varphi'\,d\varphi'\cos\theta, \quad \tau_{rz}^{F_\theta*} = \int_0^{2\pi} \tau_{rz}^{F_\theta}\, t\sin\varphi'\,d\varphi'\cos\theta \\
\tau_{r\theta}^{F_\theta*} &= \int_0^{2\pi} \tau_{r\theta}^{F_\theta}\, t\cos\varphi'\,d\varphi'\sin\theta, \quad \tau_{\theta z}^{F_\theta*} = \int_0^{2\pi} \tau_{\theta z}^{F_\theta}\, t\cos\varphi'\,d\varphi'\sin\theta.
\end{aligned}
\tag{7}
$$

Although the equations for $\sigma_r^{F_z*}-\tau_{\theta z}^{F_z*}$ are not shown in eqn (7), they are expressed with similar formula as $\sigma_r^{F_r*}-\tau_{\theta z}^{F_z*}$. The integration associated with φ' between $\varphi' = 0$ and $\varphi' = 2\pi$ are expressed with the combination of I_1–I_9 which are defined in the following equations. The integrant I_1–I_9 consist of the complete elliptic integrals of the first and second kind[11, 12]. In the following equations, $\varphi'(=\varphi-\theta)$ is replaced by a new variable φ.

$$
I_1 = \int_0^{2\pi} \frac{1}{R^3}d\varphi = C_1\frac{E}{k'^2}, \qquad I_3 = \int_0^{2\pi} \frac{\cos\varphi}{R^3}d\varphi = C_1\frac{(1+k'^2)E - 2k'^2K}{k^2k'^2}
$$

$$
I_3 = \int_0^{2\pi} \frac{\cos^2\varphi}{R^3}d\varphi = C_1\frac{(1+6k'^2+k'^4)E - 4k'^2(1+k'^2)K}{k^4k'^2}
$$

$$
I_4 = \int_0^{2\pi} \frac{\cos^3\varphi}{R^3}d\varphi = C_1\frac{(3+29k'^2+29k'^4+3k'^6)E - 2k'^2(9-14k'^2+9k'^4)K}{3k^6k'^2}
$$

$$
I_5 = \int_0^{2\pi} \frac{1}{R^5}d\varphi = C_2\frac{2(1+k'^2)E - k'^2K}{3k'^4}
$$

$$
I_6 = \int_0^{2\pi} \frac{\cos\varphi}{R^5}d\varphi = C_2\frac{2(1-k'^2+k'^4)E - k'^2(1+k'^2)K}{3k^2k'^4}
\tag{8a}
$$

$$
I_7 = \int_0^{2\pi} \frac{\cos^2\varphi}{R^5}d\varphi = C_2\frac{2(1-3k'^2-3k'^4+k'^6)E - k'^2(1-10k'^2+k'^4)K}{3k^4k'^4}
$$

$$
I_8 = \int_0^{2\pi} \frac{\cos^3\varphi}{R^5}d\varphi
= C_2\frac{2(1-5k'^2-24k'^4-5k'^6+k'^8)E - k'^2(1-33k'^2-33k'^4+k'^6)K}{3k^6k'^4}
$$

$$
I_9 = \int_0^{2\pi} \frac{\cos^4\varphi}{R^5}d\varphi
= C_2\frac{2(1-7k'^2-58k'^4-58k'^6-7k'^8+k'^{10})E - k'^2(1-68k'^2-122k'^4-68k'^6+k'^8)K}{3k^8k'^4}
$$

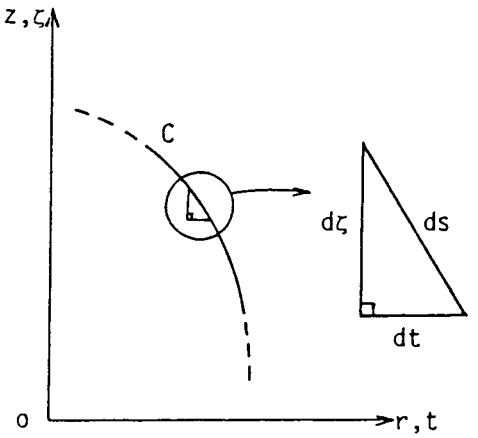

Fig. 5. The infinitestimal curved line element C where body forces are applied.

where,

$$R^2 = r^2 + t^2 + (z - \zeta)^2 - 2rt\cos\varphi \tag{8b}$$

$$C_1 = \frac{4}{\{(r+t)^2 + (z-\zeta)^2\}^{3/2}}, \qquad C_2 = \frac{4}{\{(r+t)^2 + (z-\zeta)^2\}^{5/2}} \tag{8c}$$

$$k^2 = \frac{4rt}{(r+t)^2 + (z-\zeta)^2}, \qquad k'^2 = 1 - k^2 \tag{8d}$$

$$K = \int_0^{\pi/2} \frac{d\lambda}{\sqrt{1 - k^2\sin^2\lambda}}, \qquad E = \int_0^{\pi/2} \sqrt{1 - k^2\sin^2\lambda}\, d\lambda. \tag{8e}$$

4. PROCEDURE FOR NUMERICAL SOLUTIONS

Bending problems of various axi-symmetrical bodies can be numerically solved using the fundamental solutions described in Section 3. In the present paper, the solutions for an infinite body containing a spheroidal cavity (Fig. 6) or a troidal cavity (Fig. 7) are shown.

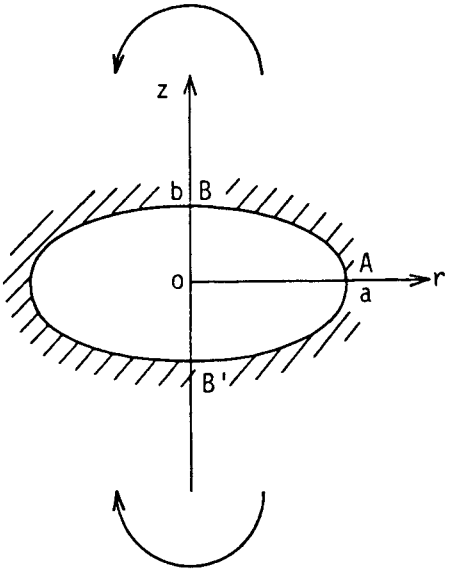

Fig. 6. A spheroidal cavity in an infinite body under bending.

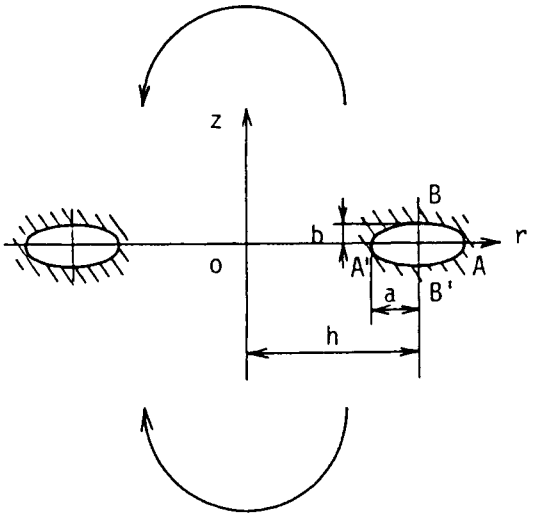

Fig. 7. A troidal cavity in an infinite body under bending.

4.1. *Definition of body force densities*

The body force densities ρ_r, ρ_θ and ρ_z distributed in r, θ and z direction are defined in eqn (9).

$$\rho_r \cos\varphi = \frac{dF_r}{t\, d\zeta\, d\varphi}, \quad \rho_\theta \sin\varphi = \frac{dF_\theta}{t\, ds\, d\varphi}, \quad \rho_z \cos\varphi = \frac{a}{t}\frac{dF_z}{t\, dt\, d\varphi}. \tag{9}$$

The definition ρ_z in eqn (9) is defined considering the bending stress field $\sigma_z = \sigma_0 r/a \cos\phi$. Defining body force densities such as eqn (9) is not forced but suitable to getting accurate numerical result.

4.2. *Solution for a spheroidal cavity*

Since the solution for this problem was given by Neuber, the accuracy of the present solution can be checked by this problem. The procedure for the analysis of a troidal cavity is almost the same as the problem of a spheroidal cavity.

4.2.1. *Dividing boundaries.* The boundary of the spheroidal cavity is divided equally after the physical plane ($r^2/a^2 + z^2/b^2 = 1$) is mapped into a circle in a mapping plane, that is, when we express the coordinate (r, z) on the ellipse by eqn (10), the angle ψ is used for the parameter indicating the division.

$$r = a\cos\psi, \qquad z = b\sin\psi. \tag{10}$$

The starting and the end points of ψ_{j1}, ψ_{j2} of the j-th division along AB in Fig. 6 are given by eqn (11).

$$\psi_{j1} = \frac{\pi(j-1)}{2n_1}, \qquad \psi_{j2} = \frac{\pi j}{2n_1}. \tag{11}$$

The boundary AB' in Fig. 6 is also divided in the same way considering the symmetry. The midpoints of each division are used for matching the boundary conditions. If we call the division where the boundary conditions are to be satisfied the i-th division, the coordinate of the midpoint of i-th division is given by eqn (12).

$$\psi_i = \frac{\pi}{2n_1}(i - 0.5). \tag{12}$$

Taking the symmetry with respect to the $z = 0$ into consideration, the same densities of the body forces should be distributed at $z = \pm\zeta$ of the j-th division.

4.2.2. *Calculation of influence coefficient.* In this paper, the stresses induced at the midpoint of the i-th division by the body force with unit density at the j-th division are called influence coefficients. We need the influence coefficients $\sigma_{ni}^{\rho rj}$, $\tau_{ni}^{\rho rj}$ etc. These stresses can be calculated by integrating (with respect to angle ψ) σ_n^{Fr*}, τ_{ni}^{Fr*}, . . . τ_{ni}^{Fz*} that are given with the fundamental solution defined in Section 3 and by eqns (3) and (4). If $\sigma_{ni}^{\rho rj}$, $\sigma_{ni}^{\rho\theta j}$ and $\sigma_{ni}^{\rho zj}$ are taken as examples, they are written like eqn (13), where the relation $d\zeta = (b/a)t\, d\psi$ and $dt = (a/b)\xi\, d\psi$ are used for rewriting.

$$\begin{aligned}
\sigma_{ni}^{\rho rj} &= \int_{\psi j1}^{\psi j2} \sigma_n^{Fr*} \frac{b}{a} t\, d\psi + \int_{-\psi j1}^{-\psi j2} \sigma_n^{Fr*} \frac{b}{a} t\, d\psi \\
\sigma_{ni}^{\rho\theta j} &= \int_{\psi j1}^{\psi j2} \sigma_n^{F\theta*} \sqrt{\left(\frac{b}{a} t\right)^2 + \left(\frac{a}{b} \zeta\right)^2}\, d\psi + \int_{\psi j1}^{\psi j2} \sigma_n^{F\theta*} \sqrt{\left(\frac{b}{a} t\right)^2 + \left(\frac{a}{b} \zeta\right)^2}\, d\psi \qquad (13) \\
\sigma_{ni}^{\rho zj} &= \int_{\psi j1}^{\psi j2} \sigma_n^{Fz*} \frac{t}{a} \frac{a}{b} |\zeta|\, d\psi - \int_{-\psi j1}^{-\psi j2} \sigma_n^{Fz*} \frac{t}{a} \frac{a}{b} |\zeta|\, d\psi
\end{aligned}$$

where (t, ζ) is the coordinate of the application of body forces in the plane $\theta = 0$. The minus sign of the second term in the third equation of eqn (13) means that the body force is applied in negative z-direction. The integration with respect to ψ is performed numerically using Simpson's rule.

4.2.3. *Determination of body force densities.* The body force densities are determined solving the following $3n_1$ linear equations which express the boundary conditions at the spheroidal surface.

$$\begin{aligned}
&\sum_{j=1}^{n1} (\rho_{rj}\sigma_{ni}^{\rho rj} + \rho_{\theta j}\sigma_{ni}^{\rho\theta j} + \rho_{zj}\sigma_{ni}^{\rho zj}) + \sigma_0 \frac{r_i}{a} \sin^2 \psi_i = 0 \\
&\sum_{j=1}^{n1} (\rho_{rj}\tau_{nti}^{\rho rj} + \rho_{\theta j}\tau_{nti}^{\rho\theta j} + \rho_{zj}\tau_{nti}^{\rho zj}) + \sigma_0 \frac{r_i}{a} \sin \psi_i \cos \psi_i = 0 \qquad (14) \\
&\sum_{j=1}^{n1} (\rho_{rj}\tau_{n\theta i}^{\rho rj} + \rho_{\theta j}\tau_{n\theta i}^{\rho rj} + \rho_{zi}\tau_{n\theta i}^{\rho zi}) = 0
\end{aligned}$$

where r_i is the r coordinate at the midpoint of the i-th division and ψ_i is the angle between the axis and the outerward normal at the same point. Once the body force densities are determined, the stresses at an arbitrary point can easily be calculated by using the body force densities and the stresses at the point due to unit body force density which can be determined from eqn (13) similarly as the influence coefficients.

4.2.4. *Special consideration on singular terms.* When the body forces are applied at the same points where the maximum stresses must be found, (5a)–(5c) become singular. In this case, the influence of the body forces must be considered specially. This analysis can be performed successfully, if we notice first the stresses at a separate point and then take the limiting expression after the closed form integration along a small boundary region on the assumption of plane strain. The result is written as eqn (15). In the equation, the notation ϵ means the small integrated region including the point of the maximum stress ($\psi = -\epsilon \sim \epsilon$).

$$\Delta\sigma_z^{\rho r} = -\frac{\nu}{1-\nu} \rho_r, \qquad \Delta\sigma_z^{\rho z} = \frac{\{3 + \nu/(1-\nu)\}\epsilon}{2\pi} \rho_z. \qquad (15)$$

As easily understood, in case of $i = j$ similar special integration must also be performed.

4.3. *Solution for a troidal cavity*

The method of analysis for a troidal cavity (Fig. 7) is similar to that for a spheroidal cavity (Fig. 6). Then, the explanations of the details of numerical procedure are saved.

Since this problems have symmetry with respect to the plane $z = 0$, the body force must be applied considering the boundaries ABA' and $AB'A'$ as a pair.

5. NUMERICAL RESULT AND DISCUSSION

Computer programs for the analysis of a spheroidal cavity and a tridal cavity were coded on the basis of the fundamental solutions and the procedure of numerical analysis described in Sections 2–4. The integral with respect to ψ in Section 4.2.2 was numerically performed by Sympson's rule with 10 dividing numbers. When the body forces are distributed along the division under consideration of boundary condition (i.e. $i = j$), or the maximum stresses at the end of major axis must be calculated, the dividing number for numerical integral was increased by 10 times as that of other case.

5.1. *Stress concentration of a spheroidal cavity*

Results of numerical analysis on a spheroidal cavities are shown in Table 1. The stress concentration factor (SCF) in the present analysis were obtained by the extrapolations of the results for two dividing number $n_1 = 6$ and 8; the results in [ ] of Table 1. The present results are in good agreement with the exact values by Neuber[13]. The error is at most about 0.07% even for the values extrapolated from $n_1 = 6$ and 8.

5.2. *Stress concentration of a troidal cavity*

No solution has been obtained for the problem of a troidal cavity with elliptical section. However, in two limiting cases (the case of very small radius of a troid and that of very large radius of a troid), the stress concentration factors can be compared with the exact solution of a three-dimensional deep hyperbolic notch and that of a two-dimensional elliptical hole. First of all, in order to check the accuracy, a few cases for

Table 1. Stress concentration factors of a spheroidal cavity in an infinite body under bending $\left(\begin{bmatrix} n_1 = 6 \\ n_1 = 8 \end{bmatrix}\right)$

	$\nu = 0$		$\nu = 0.3$	
	Present analysis	Neuber	Present analysis	Neuber
$a = 0.5b$	$1.250 \begin{bmatrix} 1.2474 \\ 1.2481 \end{bmatrix}$	1.250	$1.294 \begin{bmatrix} 1.2915 \\ 1.2921 \end{bmatrix}$	1.293
$a = b$	$1.635 \begin{bmatrix} 1.6236 \\ 1.6264 \end{bmatrix}$	1.635	$1.710 \begin{bmatrix} 1.7038 \\ 1.7053 \end{bmatrix}$	1.709
$a = 2b$	$2.460 \begin{bmatrix} 2.4337 \\ 2.4403 \end{bmatrix}$	2.459	$2.564 \begin{bmatrix} 2.5604 \\ 2.5613 \end{bmatrix}$	2.564
$a = 4b$	$4.149 \begin{bmatrix} 4.1085 \\ 4.1186 \end{bmatrix}$	4.147	$4.270 \begin{bmatrix} 4.2960 \\ 4.2895 \end{bmatrix}$	4.273

Table 2. Stress concentration factors K_{ii}^* of a troidal cavity having a very small radius of a troid in an infinite body under bending $\left(\begin{matrix} a = 2b \\ \nu = 0 \end{matrix}, \begin{bmatrix} n_1 = 16 \\ n_1 = 20 \end{bmatrix}\right)$

	Present analysis	Neuber
$c/\rho = 1.0$ $(c/a = 0.25)$	$1.285 \begin{bmatrix} 1.2628 \\ 1.2672 \end{bmatrix}$	1.292
$c/\rho = 0.5$ $(c/a = 0.125)$	$1.153 \begin{bmatrix} 1.1045 \\ 1.1142 \end{bmatrix}$	1.155

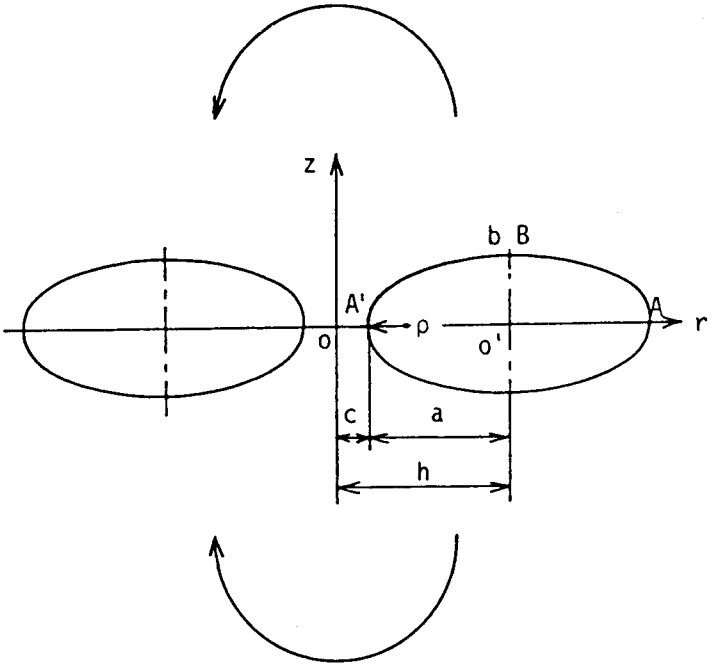

Fig. 8. A troidal cavity having a very small radius of a troid in an infinite body under bending ($\nu = 0$, $c \ll a$).

very small radius of a troid as shown in Fig. 8 were calculated. The results are shown in Table 2. The values by Neuber[14] in Table 2 are the exact SCF for three-dimensional deep hyperbolic notches. SCFs in the present analysis were determined from the maximum stress $\sigma_{\max i}$ at the inner end of major axis of troidal cavity. The bending moment M was obtained by the numerical integration of the stress $\sigma_{zi}(r)$ at the minimum section OA′ in Fig. 8. Denoting SCF at the inner end of the cavity by K_{ti}^*, we have,

$$M = 4\int_0^c \int_0^{\pi/2} \sigma_{zi}(r) r^2 \cos^2\theta \, d\theta \, dr$$

$$= \pi \int_0^c \sigma_{zi}(r) r^2 \, dr \tag{16}$$

$$K_{ti}^* = \frac{\sigma_{\max i}}{\sigma_{ni}^*}, \qquad \sigma_{ni}^* = \frac{4M}{\pi c^3} \tag{17}$$

where σ_{ni}^* is the nominal bending stress at the minimum section OA′. The extrapolations were performed using the results for the dividing numbers $n_1 = 16$ and 20 (these numbers correspond to the upper and lower values in [ ]). The present results are in good agreement with Neuber's exact solution[14] for a deep hyperbolic notch with the same values of root radius ρ.

Table 3 shows the results for other various cases. K_{to} is SCF at the outer end of the troidal cavity. The values in square brackets are the results for $n_1 = 12$ and 16 respectively and the final values were extrapolated from these results. SCF and the nominal stresses in these cases were defined as follows.

$$K_{ti} = \frac{\sigma_{\max i}}{\sigma_{ni}}, \qquad \sigma_{ni} = \sigma_o$$

$$K_{to} = \frac{\sigma_{\max o}}{\sigma_{no}}, \qquad \sigma_{no} = \sigma_o \frac{h + a}{c}. \tag{18}$$

The stress concentrations in Table 3 are plotted in Fig. 9. As $h/a \to \infty$, the calculated

Table 3. Stress concentration factors K_{ti}, K_{to} of a troidal cavity having a very large radius of a troid in an infinite body under bending $\left(\nu = 0, \begin{bmatrix} n_1 = 12 \\ n_1 = 16 \end{bmatrix}\right)$

	$a = b$		$a = 2b$	
	K_{ti}	K_{to}	K_{ti}	K_{to}
$h/a = 5$	$3.281 \begin{bmatrix} 3.2731 \\ 3.2751 \end{bmatrix}$	$2.574 \begin{bmatrix} 2.5736 \\ 2.5737 \end{bmatrix}$	$5.566 \begin{bmatrix} 5.5539 \\ 5.5569 \end{bmatrix}$	$4.283 \begin{bmatrix} 4.2835 \\ 4.2834 \end{bmatrix}$
$h/a = 10$	$3.151 \begin{bmatrix} 3.1469 \\ 3.1479 \end{bmatrix}$	$2.773 \begin{bmatrix} 2.7736 \\ 2.7734 \end{bmatrix}$	$5.298 \begin{bmatrix} 5.2916 \\ 5.2931 \end{bmatrix}$	$4.623 \begin{bmatrix} 4.6242 \\ 4.6240 \end{bmatrix}$
$h/a = 20$	$3.083 \begin{bmatrix} 3.0809 \\ 3.0814 \end{bmatrix}$	$2.887 \begin{bmatrix} 2.8877 \\ 2.8876 \end{bmatrix}$	$5.157 \begin{bmatrix} 5.1539 \\ 5.1548 \end{bmatrix}$	$4.814 \begin{bmatrix} 4.8126 \\ 4.8130 \end{bmatrix}$
$h/a = 50$	$3.037 \begin{bmatrix} 3.0354 \\ 3.0358 \end{bmatrix}$	$2.955 \begin{bmatrix} 2.9568 \\ 2.9564 \end{bmatrix}$	—	—

SCF of troidal cavities approaches the limiting value $K_t = 1 + 2a/b$ which is SCF of an elliptical hole in an infinite plate under tension. Thus, the present numerical results are in good agreement with exact solutions in the two extreme limits; $c/a \to 0$ and $h/a \to \infty$. Therefore, the high accuracy of the present analysis between these two limiting cases may be expected. Table 4 shows the numerical results for several cases between

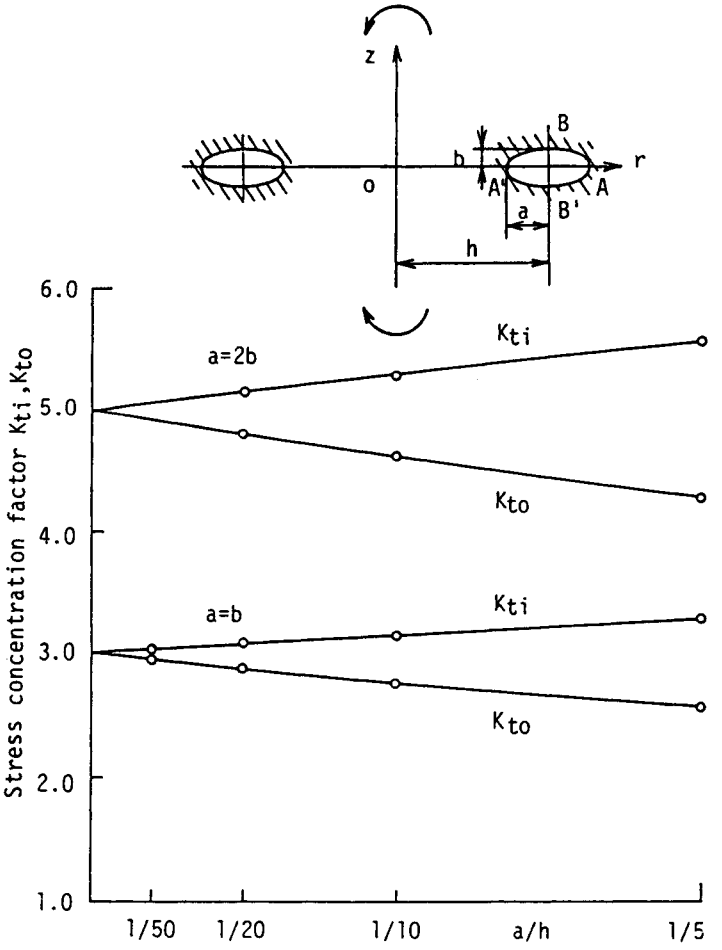

Fig. 9. Stress concentration factors K_{ti}, K_{to} for a very small radius of a troid in an infinite body under bending ($\nu = 0$, $h \gg a$).

Table 4. Stress concentration factors K_{ti}, K_{to} and K_{ti}^* of a troidal cavity in an infinite body under bending ($\nu = 0.3$)

	$a = 0.5b$	$a = b$	$a = 2b$
$h/a = 1.5$	$K_{ti} = 3.627$ $K_{to} = 1.533$ $K_{ti}^* = 1.034$	$K_{ti} = 5.418$ $K_{to} = 2.207$ $K_{ti}^* = 1.142$	$K_{ti} = 9.100$ $K_{to} = 3.582$ $K_{ti}^* = 1.508$
$h/a = 2$	$K_{ti} = 2.944$ $K_{to} = 1.597$ $K_{ti}^* = 1.074$	$K_{ti} = 4.303$ $K_{to} = 2.327$ $K_{ti}^* = 1.277$	$K_{ti} = 7.330$ $K_{to} = 3.803$ $K_{ti}^* = 1.893$
$h/a = 3$	$K_{ti} = 2.456$ $K_{to} = 1.691$ $K_{ti}^* = 1.148$	$K_{ti} = 3.671$ $K_{to} = 2.488$ $K_{ti}^* = 1.524$	$K_{ti} = 6.281$ $K_{to} = 4.093$ $K_{ti}^* = 2.443$
$h/a = 5$	$K_{ti} = 2.205$ $K_{to} = 1.792$ $K_{ti}^* = 1.297$	$K_{ti} = 3.349$ $K_{to} = 2.658$ $K_{ti}^* = 1.867$	$K_{ti} = 5.688$ $K_{to} = 4.395$ $K_{ti}^* = 3.092$

two limiting cases. Poisson's ratio is assumed $\nu = 0.3$ and the figures of four digits in the table were extrapolated using the results for $n_1 = 12$ and 16.

Although SCF of troidal cavities is not so useful itself, it has the importance from the viewpoint that the method of the analysis becomes the basis for the analysis of cylindrical bar with a circumferential notch by relieving the stresses σ_r, τ_{rz} and $\tau_{r\theta}$ at the cylindrical surface $r = h$.

6. CONCLUSION

Stress concentration problems of an axially symmetrical body under bending were solved by the body force method which has been used mainly for the analysis of plane and axi-symmetric problems. First of all, the fundamental solutions were seeked. The forms of the fundamental solutions in benidng are not so self-evident as tension and torsion problems. In order to find the necessary and sufficient forms of the fundamental solutions, the properties of the boundary conditions and those of stress fields due to ring forces were compared. It was proved that three types of the fundamental solutions are necessary and sufficient. They are two ring forces in r and z direction with the intensity of $\cos\phi$ (ϕ is angle measured from the position of σ_{max}) and one ring force in tangential direction with the intensity of $\sin\phi$. The solution can be solved numerically by superposing these three fundamental solutions. The accuracy of the numerical method was checked by solving the bending problem of a spheroidal cavity. The maximum error of the results was 0.07%. The numerical results for the bending problem of a troidal cavity approached to the exact solution in the two limiting cases of the shape of the troidal cavity. The accurate method developed for the stress concentration analysis of a troidal cavity will be extended to the stress concentration analysis of a notched cylindrical bar under bending in the second paper.

REFERENCES

1. H. Neuber, *Kerbspannungslehre*. Springer-Verlag, Berlin (1957).
2. R. E. Peterson, *Stress Concentration Design Factors*. John-Wiley & Sons, New York (1962).
3. M. Nisida, *Stress Concentration* (in Japanese). Morikitashuppan, Tokyo (1972).
4. H. Miyamoto, Three-dimensional problems in the theory of elastisity (in Japanese). *Syokabo* **10**, Tokyo (1967).
5. H. Nisitani, The two-dimensional stress problem solved using an electric digital computer. *Bull. J.S.M.E.* **11**, 14–23 (1968).
6. H. Nisitani, Solution of notch problems by body force method. In *Mechanics of Fracture*, (Edited by Sih, G. C.), Vol. 5. Noodhoff, Leyden (1978).
7. Y. Murakami and H. Nisitani, Stress intensity factor for circumferentially cracked round bar in tension. *Trans. Japan Soc. Mech. Engrs* (in Japanese) **41**, 360–369 (1975).
8. Y. Murakami, N. Noda and H. Nisitani, The analysis of stress concentration of a cylindrical bar with

a semi-elliptical circumferential notch under tension. *Trans. Japan Soc. Mech. Engrs* (in Japanese) **47,** 1194–1205 (1977).
9. H. Nisitani and K. Hashimoto, Stress concentration factors for the torsion of shafts with a circumferential semi-elliptical groove. *Trans. Japan Soc. Mech. Engrs* (in Japanese) **43,** 3642–3650 (1977).
10. S. P. Timoshenko and J. N. Goodier, *Theory of Elasticity,* 3rd ed., 390–392. McGraw–Hill, New York (1970).
11. S. Moriguchi, K. Udagawa and S. Hitotsumatsu, Mathematical formulas (in Japanese). *Iwanamishoten,* 146–149, Tokyo (1956).
12. F. Tölke, *Praktische Funktionenlehre,* Vol. 2, 88–99. Springer-Verlag, Berlin (1966).
13. pp. 120–127 in Ref. 1.
14. pp. 101–105 in Ref. 1.